UNIVERSITY OF GOTHENBURG

THE SAHLGRENSKA ACADEMY

Degree Project

Investigating Cardiac Protein Expression in two Diastolic Heart Failure Mouse Models

Petter Rudbäck

Department of Molecular and Clinical Medicine

Gothenburg

Degree project:	30 credits
Program:	Program in Medicine
Year:	2021
Supervisor:	Associate professor Stephan Lange and Assistant Professor Emma Börgeson

Table of contents

List of abbreviations

HFpEF - Heart Failure with preserved Ejection Fraction
HFrEF - Heart Failure with reduced Ejection Fraction
L-NAME - L-N^G-Nitro arginine methyl ester
NO – Nitric Oxide
HFD – High fat diet
HFL – High fat diet and L-NAME
SFD – Standard fat diet
GLS – Global longitudinal strain
dKO – Double knockout
SR – Sarcoplasmic reticulum

Abstract

Investigating Cardiac Protein Expression in two Diastolic Heart Failure Mouse Models

Author:	Petter Rudbäck
Degree project thesis:	30 credits
Program:	Program in Medicine
Year:	2021
Supervisor:	Associate Professor Stephan Lange, Assistant Professor Emma Börgeson

Key words:	HFpEF, Diastolic heart failure, Mouse model, Protein expression.

Introduction / Background: The treatment of heart failure with preserved ejection fraction (HFpEF) remains challenging as common heart failure drugs fail to reduce mortality in the patient group. There is a lack of knowledge of what molecular mechanisms are responsible for the disease and a lack of animal models to emulate the disease. There are however two new HFpEF mouse models, the High Fat diet + L-NAME (HFL) mouse model and the Obscurin/Obsl1 dKO model.

Aim(s) / Objective(s): To investigate the expression profile of key structural, metabolic and sarcoplasmic reticulum (SR) proteins in the HFL mouse model and to compare the results with previous unpublished results from the Obscurin/Obsl1 mouse model.

Methods: The concentration of 24 different proteins in 3 female and male controls as well as 3 female and male HFL mice were investigated using western blotting. The blots were then quantified using the computer program Fiji and analyzed using SPSS. The localization of Obscurin, Obsl1 and smooth muscle actin inside the tissue was visualized using immunofluorescence.

Results: In female HFL mice, a statistically significant decrease of Obscurin and an increase of Obsl1 was seen. No change was seen in male mice. For metabolism, protein changes that

indicate a metabolic switch to increased fat metabolism was seen. In the sarcoplasmic reticulum (SR) there were significant changes calcium handling proteins.

Conclusion(s) / Implication(s): Both models saw changes to SR proteins, but the specific proteins affected differed between the models. However, there are signs that both SR function and the expression of structural proteins Obscurin and Obsl1 are affected in the disease and could be underlying mechanisms. The metabolic profile on the other hand does not seem to be altered in any specific way in the disease.

Background

In 2015-2018, 2.1% of the population in the United States of America had heart failure. Today, it is the leading cause of hospitalization among the elderly. The annual 809,000 heart failure related hospital admissions cost the American healthcare system an estimated $30.7 billion. (2, 3) Approximately half of these heart failure admissions are diastolic heart failures, which is also known as heart failure with preserved ejection fraction (HFpEF). HFpEF patients show all signs of heart failure while presenting with preserved baseline ejection fraction, which is what percentage of the blood volume in the heart that gets ejected into the aorta with each heart stroke. The limit set for a preserved ejection fraction is 50% and above. Patients with systolic heart failure (or heart failure with reduced ejection fraction - HFrEF) are characterized by an ejection fraction that falls below 40%. In the middle we have heart failure with a mildly reduced ejection fraction (HFmrEF) of 40-49%. (4, 5) The clinical phenotypes of the diseases are similar, and common symptoms exhibited by patients include exercise intolerance, dyspnea, fatigue, edema, abnormal heart rhythm and lung rales. However, research suggest that there are separate pathophysiological mechanisms underlying HFpEF and HFrEF which supports a binary model of the disease. (3)

The binary model of heart failure

This binary model of heart failure is based on the tendency of HFpEF and HFrEF to affect different patient populations. HFpEF patients tend to be older (74 compared to 70 years old), have more comorbidity with hypertension (74% compared to 65%) and to be less connected to coronary disease (46% compared to 58%). The largest difference between the groups is gender, with 63% of HFpEF patients being female compared to 38% in the HFrEF group. There is also a clear bimodal curve when examining the ejection fractions of the combined patient populations with one incidence maximum at an ejection fraction of 60-65% (HFpEF) and another one at around 20-30% (HFrEF). Since the curve isn’t bell shaped the implication is that there are two different diseases in the population. Furthermore, while survival for HFrEF has improved over the past 2 decades there has been a no improved mortality for patients with HFpEF. Evidence-based medications used for treatment of HFrEF such as

Candesartan and angiotensin converting enzyme inhibitors has failed to show reduced mortality or hospitalization rates in patients with HFpEF. Results of beta blocker therapy on HFpEF have shown varying results with one observational study on women showing increased hospitalization rates if they received treatment with beta blockers. (3) However, recent research show that SGLT2-inhibitors, often used to treat type 2 diabetes, has effect in reducing hospitalizations and mortality in HFpEF patients. (6)

However, this binary model of heart failure is still under debate. It has been argued that HFpEF and HFrEF are in fact overlapping phenotypes of the same disease, and that heart failure is a spectrum of overlapping phenotypes making heart failure a multifactorial disease. There are signs of systolic and diastolic failure in both HFrEF and HFpEF and systolic dysfunction is prevalent during exercise in HFpEF. The binary heart failure model is based on biased data from the 80s where only the patients with an EF below 40% were selected to increase the statistical power. Studies were later made on the remaining heart failure population which showed less response to pharmaceutical products, but differences in characteristics and clinical response are not surprising when comparing two different extremes of a population. Some studies have also shown that the distribution of left ventricular ejection fraction could be bell-shaped (7).

Whether or not HFpEF represent a separate disease process or a different phenotype of HFrEF there is a need for research that further investigate the underlying mechanisms. The research process has however been complicated by a lack of HFpEF animal models, but recently two promising animal models has emerged as potential ways to further investigate HFpEF.

The two-hit obese and hypertensive mouse model

The high fat diet (HFD) + L-N^G-Nitro arginine methyl ester (L-NAME) model for HFpEF developed by Schiatarella and others combines two different pathological mechanisms to induce diastolic heart failure in mice. At 8 weeks old the mice were randomized to receive

eighter high fat diet (60% of kilocalories from LARD (fat)), L-NAME (0.5g/L in drinking water), a combination of both treatments or as a control group with normal food and water. The high fat diet induced glucose intolerance and obesity in the HFD group. L-NAME is a drug which inhibits nitric oxide synthetase, resulting in less available nitric oxide (NO) in blood vessels. As nitric oxide is a potent vasodilator, the lowered concentration of NO in turn leads to less relaxation of the vessels and higher blood pressure and cardiac load. Therefore, as expected, mice with L-NAME in drinking water had both systolic and diastolic blood pressure increased. Mice being fed HFD + L-NAME resulted in similar results and had both glucose intolerance, obesity and high blood pressure. (8)

The study showed that left ventricular ejection fraction was preserved in all groups. It also looked at an emerging sensitive factor for left ventricular dysfunction, left ventricle global longitudinal strain (GLS). It is defined by the relative change of longitudinal length in the systolic phase of the left ventricular myocardium compared to the original diastolic length.(8, 9) HFD + L-NAME mice showed significantly increased GLS compared to the other groups. They also showed reduced running distance in an exercise exhaustion test and increased ratio between wet and dry lung weight indicating the mice had developed heart failure associated pulmonary congestion, accumulation of fluid in the lungs. The ratio of heart weight relative to tibia length in the HFD + L-NAME group was also significantly increased, indicating an increase of heart mass. In summary the mice had signs of exercise intolerance, left ventricle dysfunction, increased cardiac mass and pulmonary congestion/edema while also having a preserved ejection fraction suggesting that this is a promising HFpEF mice model. (8)

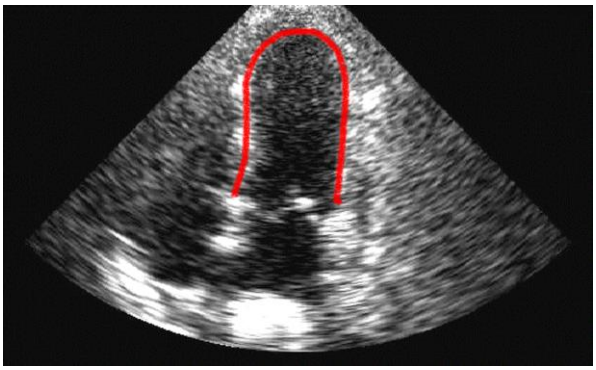

Figure 1 | Marked in red is the longitudinal length of the left ventricle in an ultrasound image, which is used as an indicator of the global longitudinal strain (GLS). (Image source (1))

The Obsl1/Obscurin double knockout model for HFpEF

Obscurin together with Titin and Nebulin are the three giant muscle-specific proteins important in sarcomere organization. The two binding sites of Obscurin are titin located in the sarcomere and small-ankyrin, a protein embedded in the sarcoplasmic reticulum. (10) Obscurin was therefore suspected to have a vital role in the structural organization of the sarcoplasmic reticulum and its relation to the sarcomere. The sarcoplasmic reticulum has the function of calcium release, reuptake and storage inside the cell. Calcium is in turn is important for myosin's binding to actin in the sarcomere and therefore the contractility of the heart. Stephan Lange and others generated a mouse Obscurin knockout to further study the function of the protein and surprisingly found that the structure and physiology of the sarcomere and sarcoplasmic reticulum (SR) was seemingly unchanged despite the loss of Obscurin. It was suspected that the protein Obsl1, a close homolog of Obscurin, was able to functionally replace Obscurin which resulted in only modest pathology in the Obscurin knockout mice. (11)

To test this hypothesis skeletal muscle and cardiac specific Obsl1 knockout and Obscurin/Obsl1 double knockouts were generated. In humans, mutations in Obsl1 that appear to result in loss of function of the gene result in 3M-growth syndrome. (12) This syndrome is characterized by postnatal growth restrictions and triangular face, prominent forehead and flat maxillae. (13) However, when global Obsl1 knocked mice were generated, the animals died prenatally before embryonic day 8. It was therefore not possible to generate a global (whole body) double knockout (dKO) of Obscurin/Obsl1 in mice. This problem was circumvented by creating skeletal and cardiac specific Obscurin/Obsl1 dKO. Skeletal muscle specific dKO mice for Obscurin/Obsl1 present with altered SR, metabolic differences and weakened sarcolemma (12). Cardiac specific dKO mice are still being investigated. Preliminary data from the laboratory indicate that cardiac Obscurin/Obsl1 dKO die prematurely starting from 12 months onward (Figure 2A). Systolic function (Figure 2B) and gross cardiac morphology (Figure 2C) showed no major differences between dKO, single Obscurin or Obsl1 knockouts and control (CTL) mice. However, hemodynamics analyses indicated that dKO mice present with profound diastolic dysfunction (Min dP/dt; pressure development during cardiac relaxation) and relaxation problems (Tau; time variable for relaxation) at baseline (no

Dobutamine; Figure 2D), indicating diastolic heart failure in these mice. Upon cardiac stress elicited by increased Dobutamine concentrations, dKO mice also show differences in systolic function (Max dP/dt; pressure development during cardiac contraction) as well as a lack in cardiac reserve.

On the molecular level, dKO mice display abnormalities in SR handling, metabolism and mitochondrial function and architecture (Figures 2E-G), similar to loss of Obscurin/Obsl1 in skeletal muscles (12). Of specific interest were changes to glycolytic enzymes (hexokinase [HK] and phosphofructokinase [PFK]) as well as Pyruvate dehydrogenase (PDH) phosphorylation, which indicate a switch from beta-oxidation (burning of fatty acids) and utilization of glucose as primary fuel for the cardiac contraction.

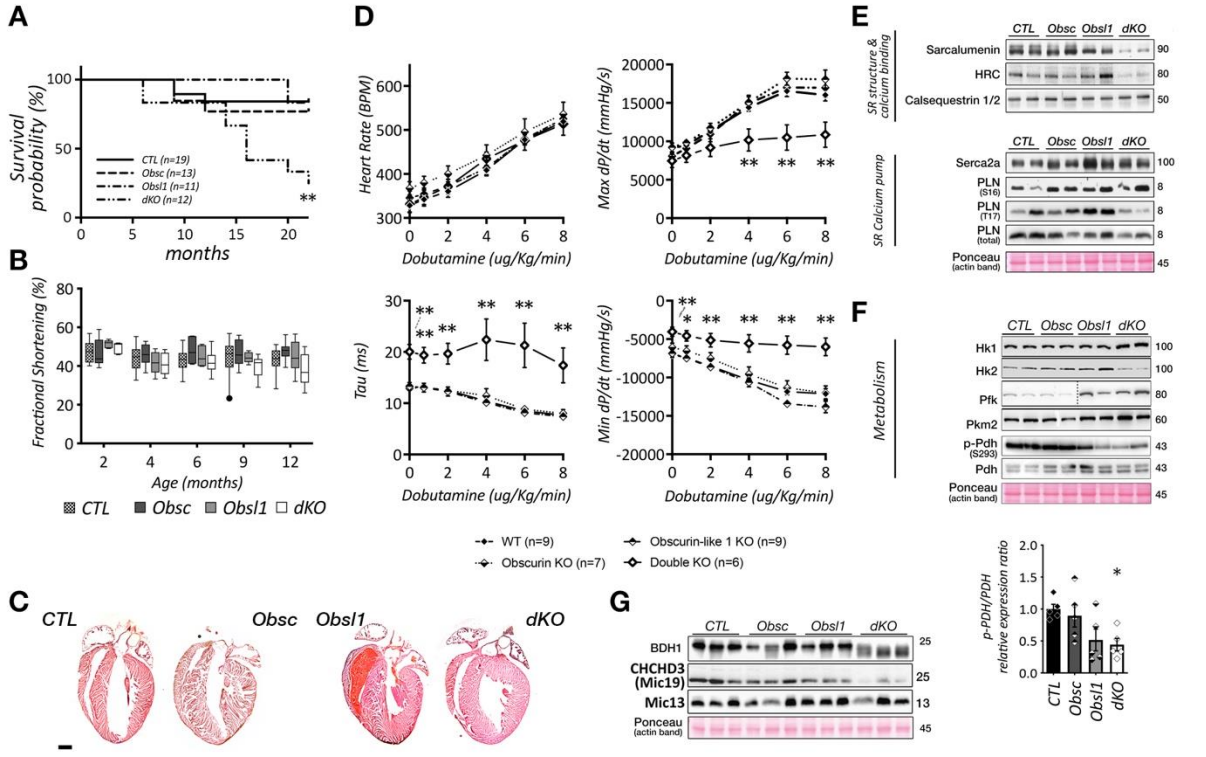

Figure 2 | **Unpublished results from Lange and others Obscurin/Obsl1 dKO HFpEF mouse model. A.** Kaplan-Meier Survival probability curve for control (CTL), single cardiac specific Obscurin and Obsl1 knockout mice and dKO mice. **B.** Fractional shortening as determined by echocardiography. **C.** Histological analysis of hematoxylin-eosin stained four chamber views of CTL, single and dKO mouse hearts. **D.** Hemodynamics analysis of CTL, single and dKO mice at baseline or with increasing amounts of the adrenergic agonist Dobutamine. **E.** Immunoblot analysis of sarcoplasmic reticulum (SR) proteins involved in structure and Calcium binding (top panel) and the SR pump Serca2 (bottom panel). **F.** Immunoblot analysis of glycolytic enzymes hexokinase 1 and 2 (HK1 and HK2), phosphofructokinase (Pfk), Pyruvate kinase (Pkm2) and pyruvate dehydrogenase alpha 1 (PDH) as well as the PDH phosphorylation level (Ser 293). Quantification of PDH phosphorylation (bottom panel) **G.** Analysis of mitochondrial enzymes involved in ketone metabolism (BDH1) and cristae formation (CHCHD3 and Mic13). Unpublished data.

Aim and Specific Objectives

Aim 1

The first aim is to investigate the cardiac expression levels of 24 different proteins between mice fed high fat diet mice also fed L-NAME according to the method developed by Schiattarella et al. (8) against healthy controls.

The gender of the mice will also be used as an independent factor, as the severity of the disease differ between the genders. The results will be compared with the unpublished data of protein levels of the OBSL/Obscurin double knockout mouse model developed by Lange et al. By analyzing the levels of these key proteins, the goal is to gain further insight into what cellular functions are failing in HFpEF. By comparing two models it is possible to more accurately pinpoint what mechanisms is disease specific and what mechanisms only would be present in one of the models. The strength and weaknesses of the models could therefore also be better understood.

Aim 2

The second aim is to investigate the locations of Obscurin, Obsl1 and smooth-muscle actin inside the cell using immunofluorescence analysis in the high fat diet + L-NAME model and in healthy controls.

The objective of comparing the subcellular localizations of the proteins is to gain more insight into how the cell gets remodeled in the disease and what cellular structures get affected. By combining the analysis of expression levels and localization analysis inside the cell we can not only compare concentrations between High fat diet + L-NAME mice and controls but also see where in the cell this concentration change is happening.

Materials and Methods

Generation of the high-fat diet and L-NAME induced HFpEF mouse model

20 mice male and 20 female mice of the strain C57BL/6 that were 8 weeks of age were randomly assigned into 4 groups. 10 male and 10 female mice were fed with standard fat diet (SFD; 10% kcal from fat), while 10 male and 10 female mice being fed high fat diet (60% kilocalories coming from fat (lard)) and L-NAME (0.5 g/l in drinking water) for 16 weeks. This method to induce a HFpEF-like phenotype in mice was first developed and characterized by Schiattarella and co-authors, and is considered the gold-standard animal model for this disease. (8) Tissues from all mice were harvested at 24 weeks of age. Hearts were collected, cut into pieces and snap-frozen in liquid nitrogen for subsequent protein analysis, and one piece of the heart was embedded in optimal cutting temperature compound (OCT) embedding medium and frozen on a block of dry ice.

Analysis of cardiac protein levels

For protein analysis, samples from 3 mice per group were randomly selected. Each of the heart samples, both from the standard fat diet (10% fat in chow) (SFD) group and the High fat diet + L-NAME (HFL; 60% fat in chow) group, were transferred into a 5ml Falcon round bottom FACS tube. 1 ml sample buffer was added to the heart sample, and tissues were homogenized using a polytron blade. The samples were then heated to 90 degrees Celsius for two minutes using a heating plate to help further denature the proteins. For normalization of protein levels, a 10% Acrylamide gel was prepared in advance and 5µl of each heart sample was added. Gel electrophoresis was performed for 110 minutes, running at constant 120V. The gel was then stained for proteins using Coomassie blue, with the gel left to rest in the staining solution overnight on a rocking platform. Subsequently, the gel was washed first

using tap water and then Coomassie destain solution for 2 hours using a shaker. It was then scanned and analyzed using the computer program Fiji [NIH Image] to perform densitometry that quantifies the intensity of the actin band in the gel (Figure 3). The intensity of the bands was used to normalize the protein levels, using the SFD.15 mouse heart sample as control. Loading volumes were normalized so that there was an equal amount of actin in each well for the next electrophoresis (Table 4).

To further fine-tune the generated loading volumes another gel was run using the newly established loading volumes for each sample (Table 4, "Second loading volume"). The proteins were then electroblotted from the gel to a nitrocellulose membrane. The membrane was then blocked with 5% BSA in Tris-buffered saline solution containing Tween-20 (TBST) incubated with a primary antibody generated in mice against cardiac actin overnight at 4ºC. It was then washed and incubated with a secondary antibody for 1 hour at room temperature that was linked to horseradish peroxidase (HRP). After repeated washing, a chemiluminescent HRP substrate (Pierce) was added and the stained bands were recorded using a Biorad Gel Imager. Actin-stained bands were quantified using densitometry and final loading volumes were generated using the results.

Using the final loading volume to get equal amounts of protein, gels were loaded with cardiac samples from male and female SFD and HFL mice. A range of acrylamide concentrations were used to make gels: 15% acrylamide gels were used for analysis of smaller proteins (<35 kDa), 10% acrylamide gels were used to investigate proteins between ~25 kDa to 150 kDa, while 8% acrylamide gels were used for the analysis of the larger proteins (ie. >150 kDa). In the next step the gels were run in a transfer electrophoresis with a nitrocellulose membrane which made the proteins migrate from the gel onto the membrane. The membrane was then reversibly stained with Ponceau to confirm the successful transfer of the proteins. Ponceau stained membranes were scanned and the images saved for future reference. The nitrocellulose membrane was then incubated in blocking solution for a minimum of 2 hours on a rocking platform. The membrane was then moved to a solution containing blocking solution and a primary antibody directed against a specific protein, which was different for every membrane (Table 1-3). The membrane was incubated in the antibody at 4ºC degrees overnight on a shaking platform. Following incubation, unbound antibodies were washed out

for three times 10 minutes using TBST solution. The membrane was then incubated with the secondary chemiluminescent antibody linked to an HRP enzyme dissolved in blocking solution for 1 hour at room temperature. Finally, the membrane was washed six times for 10 minutes, after which the membrane was exposed to SuperSignal West Pico Plus Chemoluminescent substrate (Pierce). Pictures were taken using variable exposure times on a Biorad Gel Imager. The luminescence was quantified using densitometry with the program Fiji and the results between the groups were statistically analyzed using ANOVA tests on gels with four groups (SFD male, SFD female, HFL male and HFL female) and using T-tests to compare gels with only two groups (SFD male and HFL male or SFD female and HFL female).

Table 1 | Metabolic proteins analyzed

Full name	Abbreviation	Function	Antibody used
Pyruvate dehydrogenase	PDH	Enzyme linking glycolysis to TCA (Krebs) cycle	Cell Signaling, Antibody #2784
Phosphorylated pyruvate dehydrogenase	p-PDH	Inactive form of PDH	Cell Signaling, Antibody #31866
Hexokinase 1	Hk1	Glycolytic enzyme	Cell Signaling Antibody #2804
Hexokinase 2	Hk2	Glycolytic enzyme	Cell Signaling, Antibody #2106
Pyruvate kinase M 1&2	PKM 1/2	Glycolytic enzyme	Cell Signaling, Antibody #3186
Medium-chain specific acyl-CoA dehydrogenase, mitochondrial	Acadm	Beta-oxidation	Proteintech, Antibody 55210-1-AP
Annexin A6	Anxa6	Calcium dependent phosphor-lipid binding protein at the cell membrane	Proteintech, Antibody 12542-1-AP
D-beta-hydroxybutyrate dehydrogenase	BDH	Ketone metabolism	Proteintech, Antibody 15417-1-AP
Carnitine O-palmitoyltransferase 2	CPT2	Beta-oxidation	Proteintech, Antibody 26555-1-AP
Sorting and assembly machinery 50	Sam50	Mitochondrial structure	Sigma, Antibody WH0025813M4
Coiled-coil-helix-coiled-coil-helix domain containing protein 3	CHCHD3	Mitochondrial structure	Sigma, Antibody SAB2501731
Oxidative phosphorylation proteins	Oxphos	Electron transport chain	Abcam, Antibody ab110413

Table 2 | Structural proteins analyzed

Full name	Abbreviation	Function	Antibody used
Obscurin	Obsc	Giant sarcomeric signaling protein	Custom produced, Lange lab, UCSD
Obscurin-like protein 1	OBSL1	Structural protein	Abcam, Antibody ab204075
Striated muscle preferentially expressed protein kinase	SPEG	Muscle cell cytoskeletal protein	Sigma, Antibody HPA018904
EH-Myomesin	-	Sarcomeric structure	Custom produced, Perriard lab ETH Zurich
Smooth muscle actin	SMA	Myofibroblast protein	DAKO, Antibody M085129-2

Table 3 | Proteins analyzed associated with the Sarcoplasmic Reticulum

Full name	Abbreviation	Function	Antibody used
Sarco/endoplasmic reticulum calcium (Ca2+) ATPase cardiac isoform	Serca2a	Calcium reuptake into the SR	Alomone, Antibody ACP-012
Phospholamban	PLN	Inhibitor of Serca2a	Badrilla, Antibody A010-14
Phospholamban phosphorylated at threonin17	PLN-T17	Inactivated PLN	Badrilla, Antibody A010-13
Sarcalumenin	-	Calcium binding inside the SR	DSHB, Antibody XIIC4
Sarcoplasmic reticulum histidine-rich calcium-binding protein	HRC	Calcium storage, release and reuptake	Sigma, Antibody HPA004833
Calsequestrin	-	Calcium storage buffer	Abcam, Antibody ab185220
X-box binding protein 1	Xbp1	Cell stress transcription factor	Cell Signaling, Antibody #12782

Analyzing the subcellular localization of proteins

One male and one female left ventricle from mice on either a standard fat diet (chow) or from on high fat diet with L-NAME added to drinking water were slowly frozen (-80 degrees Celsius) in Optimal Cutting Temperature (OCT) solution. The samples were then put in to a cryotome and 14µm thick slices of the ventricle were cut. The slices were then mounted to a positively charged microscope glass slide (Fisher Scientific). They were arranged pairwise with 8 pairs on each slide. Slides were stored at -80ºC before staining.

For staining, the slides were first immersed in acetone at -20 degrees Celsius for 5 minutes to fixate the samples. They were then immersed in phosphate buffered saline in room temperature for 5 minutes to rehydrate sections. Next was a cell membrane permeabilization step where the slides were immersed in phosphate buffered saline containing 0.2% of Triton, a detergent. The slides were then covered with 5% donkey serum in gold buffer for 1 hour at room temperature in a humid chamber to block unspecific binding sites. Primary antibodies dissolved in gold buffer were then added to the slides. For each pair two different antibodies were added, one produced in mice, and one produced in rabbits. The combinations of antibodies were different for each pair. The slides were kept in 4 degrees Celsius overnight in a humid box. They were then washed three times for five minutes with phosphate buffered saline before the secondary antibodies dissolved in gold buffer were added to the slides. The secondary fluorescently labeled antibodies as well as DAPI to label nuclei and fluorescently linked phalloidin to label filamentous actin were added to each pair on the slides. Subsequently, slides were incubated for 1 hour at room temperature in a humid box, after which unbound antibodies were washed off the sections using phosphate buffered saline for 3 times for ten minutes each. Following washes, sections were mounted using DAKO fluorescent mounting medium and stored at 4ºC until imaging.

Imaging was done in sequential scanning mode on a Leica TCS-SP laser scanning microscope, equipped with a 20x air objective and an 63x oil immersion objective, and zoom rates between 1 and 2. Images were analyzed using Fiji.

Students Contribution

During the study I have collected all the data from the High fat diet/L-NAME mice and controls, both by running western blots and also by preparing immunofluorescence slides and images for presentation. By using SPSS and ImageJ I also did statistical analysis of the results. The results from the Obscurin/OBSL1 double knockout mice used in this thesis was preexisting data and not collected by me.

Ethics

The use of mice in this study was approved by The Institutional Animal Care and Use Committee (IACUC), University of California, San Diego, protocol No. S13009. All animals always had food and water available and were euthanized if there were signs of distress.

It was necessary to use an animal model in these experiments since immunofluorescence analysis has to be prepared with live animals and since there was a need to have both genetically and environmentally identical animals on which to do the experiments on.

Results

Generation of loading volumes

The gel loaded with 5 µl loading volumes and stained with Coomassie blue (Figure 3a) generated the second loading volumes (Table 4) after normalization of actin using densitometry. The secondary loading volumes used on a western blot with an antibody against cardiac actin (Figure 3b) generated the final loading volumes (Table 4) used in all subsequent western blots.

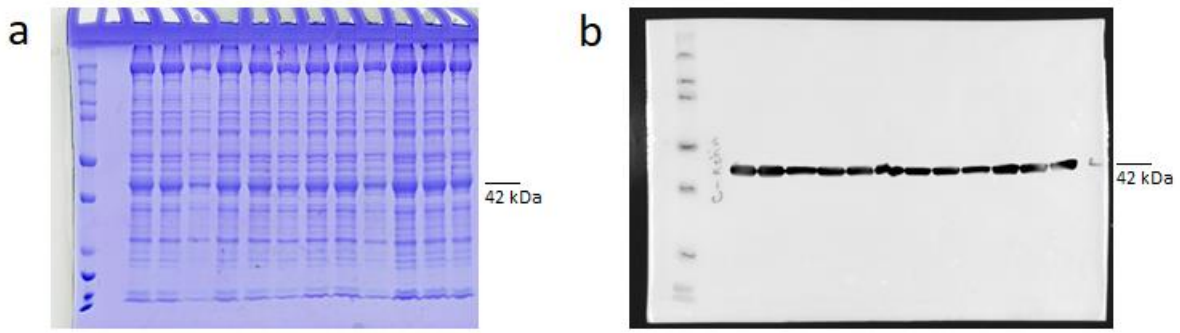

Figure 3 | **Normalizing protein levels according to c-actin levels in each sample. a**, A gel loaded with 5 µl of samples SFD-M-1 to HFL-F-3 according to table 4. The actin band is marked as 42 kDA. **b**, Western blot marked with an antibody against cardiac actin used in generating the final loading volumes in Table 4.

Table 4 | Chart of the loading volumes for each of the samples. SFD - Standard fat diet, HFL - High fat diet + L-NAME, M - Male, F - Female.

Sample name	Original loading volume (µl)	Second loading volume (µl)	Final loading volume (µl)
SFD-M-1	5.0	3.5	3,26
SFD-M-2	5.0	3.9	3,26
SFD-M-3	5.0	7.3	7,30
SFD-F-1	5.0	3.8	3,66
SFD-F-2	5.0	3.9	3.97
SFD-F-3	5.0	5.0	4.63
HFL-M-1	5.0	3.5	3,62
HFL-M-2	5.0	3.4	3,62
HFL-M-3	5.0	5.1	6,19
HFL-F-1	5.0	3.1	3,10
HFL-F-2	5.0	3.6	4,08
HFL-F-3	5.0	4.3	4,81

Structural cardiac and fibrotic marker proteins

We investigated the following sarcomeric proteins that are important for the structure of the sarcomere: the obscurin family proteins obscurin, Obsl1 (obscurin-like 1) and SPEG (striated muscle preferentially expressed gene), as well as EH-myomesin, an isoform of myomesin-1. We also tested levels of smooth-muscle actin, a marker for activated myofibroblasts that becomes active in myocardial fibrosis leading to interstitial fibrosis.

The level of obscurin in female HFL mice were significantly (p=0.044) lower (41% of SFD) compared to healthy female mice (Figure 4, Figure 5). No significant change in obscurin level was found in male mice. Using 20x magnification in immunofluorescence images, no clear difference in the ultracellular distribution of the protein was found in any group (Figure 6). For OBSL1, female HFL mice had a significant (p=0.009) increase (188% of SFD) compared to healthy female mice (Figure 4, Figure 5). No significant difference was seen in male mice OBSL1 levels (Figure 4, Figure 5) or in the ultracellular distribution in immunofluorescence analysis (Figure 7). No significant change in protein levels were seen for SPEG, Smooth muscle actin and EH-myomesin (Figure 4, Figure 5). In immunofluorescence analysis of smooth muscle actin there were no signs of fibrosis in cardiac tissue compared to controls (Figure 8). Smooth muscle actin was only observed surrounding the cardiac vasculature. 60x magnification of obscurin in female mice showed that in both female HFL and SFD mice Obscurin was localized in between the actin bands in a striated pattern.

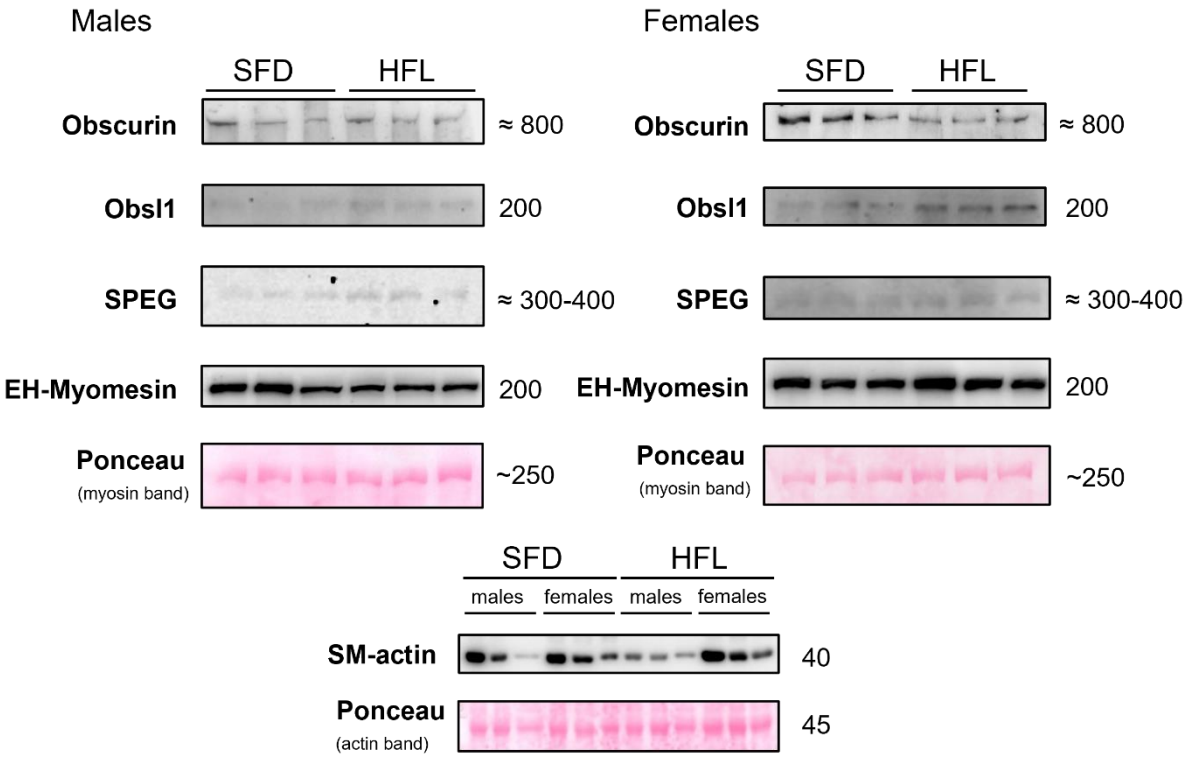

Figure 4 | **Western blots of the structural proteins.** The images have been cropped to only include the relevant bands with the molecular weight (Kilodaltons) of the protein to the right of the blot. Darker bonds correspond to a higher concentration of the protein in the sample in correlation to cardiac actin. The proteins analyzed are Obscurin, Obscurin-like protein 1 (Obsl1), Striated muscle preferentially expressed protein kinase (SPEG), EH-Myomesin and smooth muscle actin (SM-actin) with the molecular weight of the proteins in kilodaltons on the right. SFD - Standard fat diet, HFL - High fat diet + L-NAME. Ponceau stained actin or myosin bands are shown as loading control.

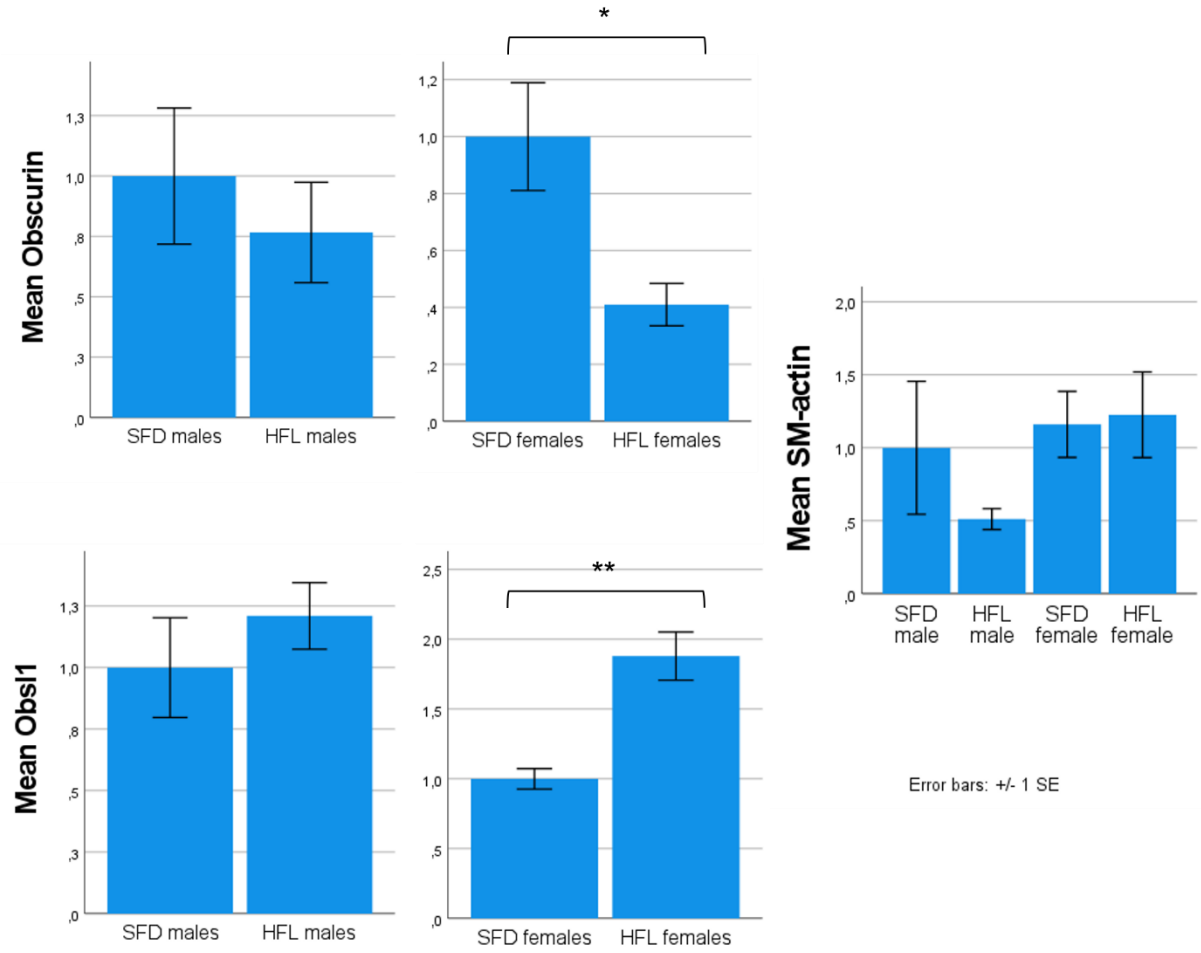

Figure 5 | Quantified values of the immunoblots in Figure 4 presented in bar graphs. Obsl1 = Obscurin like protein 1, SM-actin = Smooth muscle actin. *p<0.05, **p<0.01.

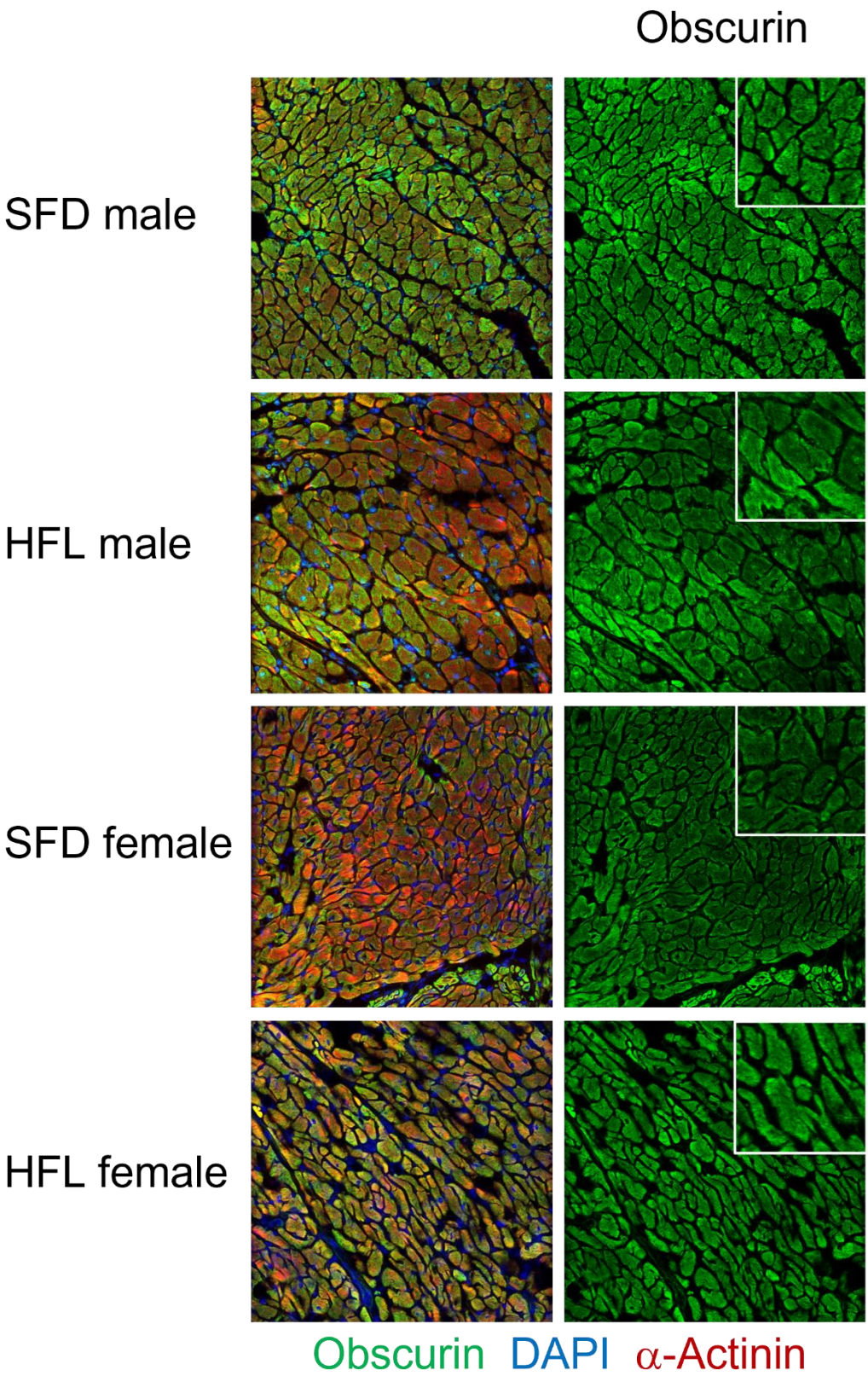

Figure 6 | **20x Immunofluorescence images of Obscurin in cardiac tissue.** Each color corresponds to a different structure stated at the bottom of the figure. 4′,6-diamidino-2-phenylindole (DAPI) is a stain that binds to the nucleus and α-actinin is a cytoskeletal protein. On the left is all colors combined and on the right is only Obscurin with a magnified image in the top right. SFD – Standard fat diet mice (controls) HFL – High fat diet + L-NAME mice (test group)

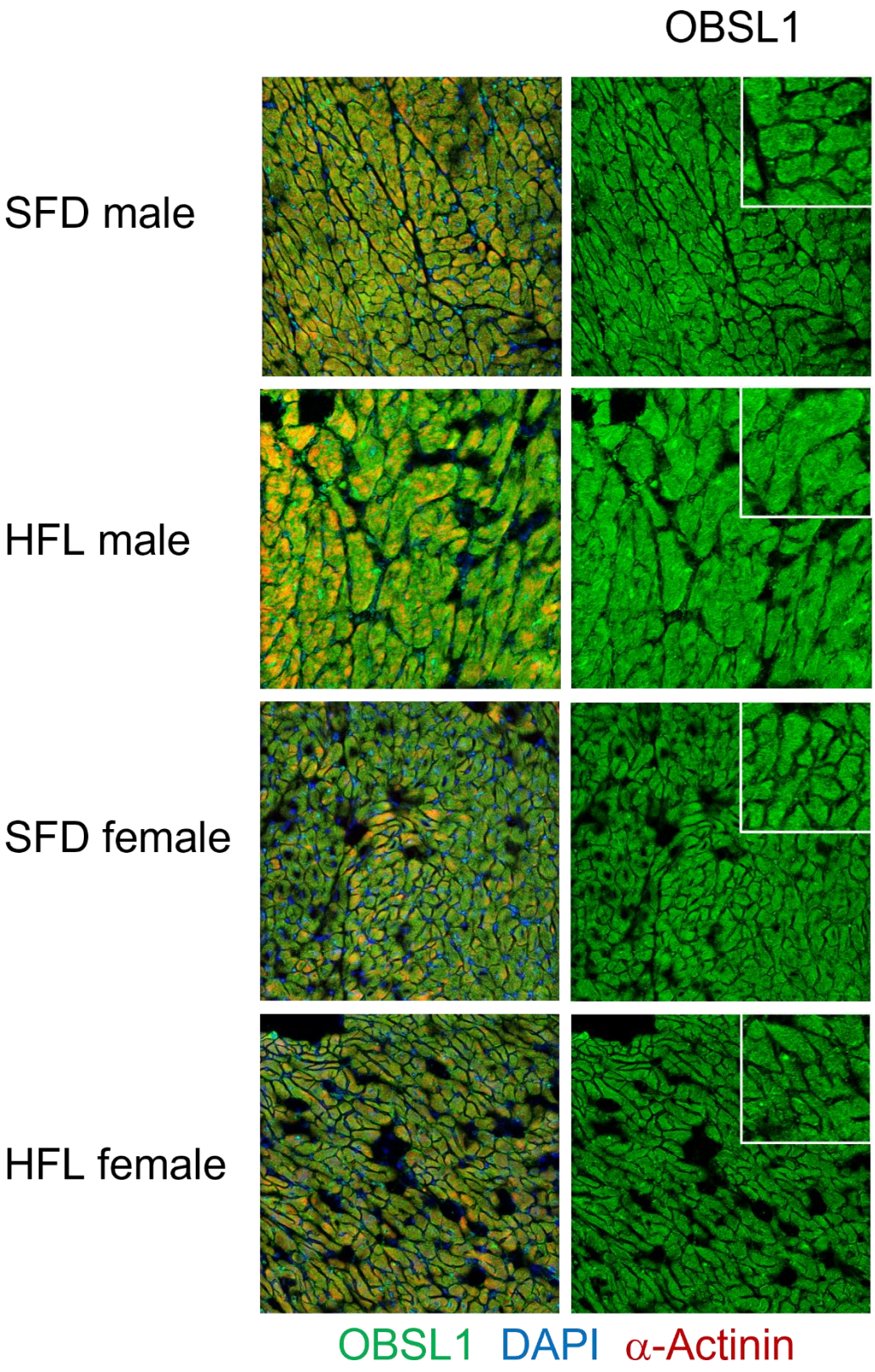

Figure 7 | **20x Immunofluorescence images of Obsl1 in cardiac tissue.** Each color corresponds to a different structure stated at the bottom of the figure. 4′,6-diamidino-2-phenylindole (DAPI) is a stain that binds to the nucleus and α-actinin is a cytoskeletal protein. On the left is all colors combined and on the right is only Obsl1 with a magnified image in the top right. SFD – Standard fat diet mice (controls) HFL – High fat diet + L-NAME mice (test group)

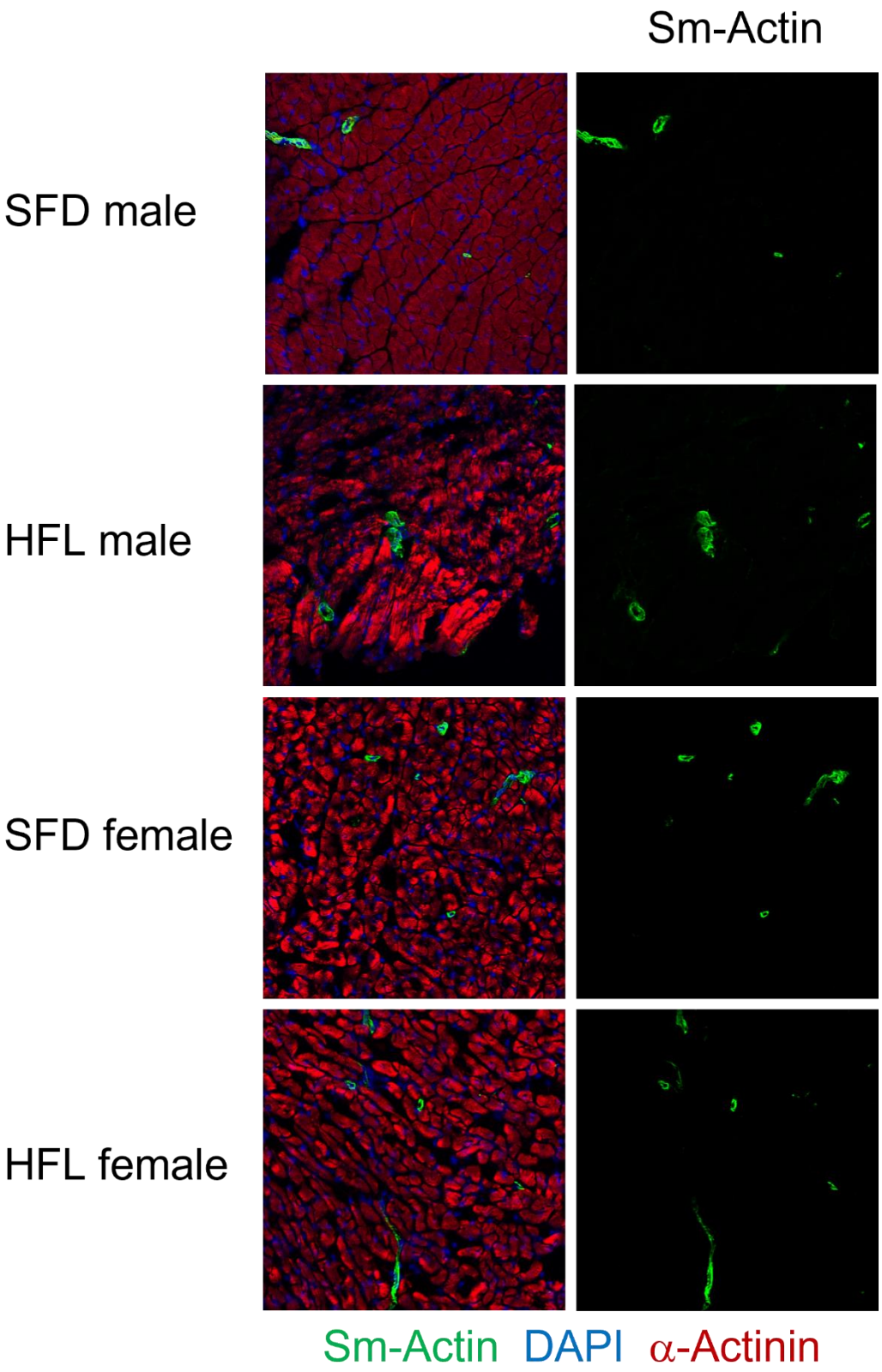

Figure 8 | **20x Immunofluorescence images of Smooth muscle actin (SM-actin) in cardiac tissue.** Each color corresponds to a different structure stated at the bottom of the figure. 4′,6-diamidino-2-phenylindole (DAPI) is a stain that binds to the nucleus and α-actinin is a cytoskeletal protein. On the left is all colors combined and on the right is only SM-actin with a magnified image in the top right. SFD – Standard fat diet mice (controls) HFL – High fat diet + L-NAME mice (test group).

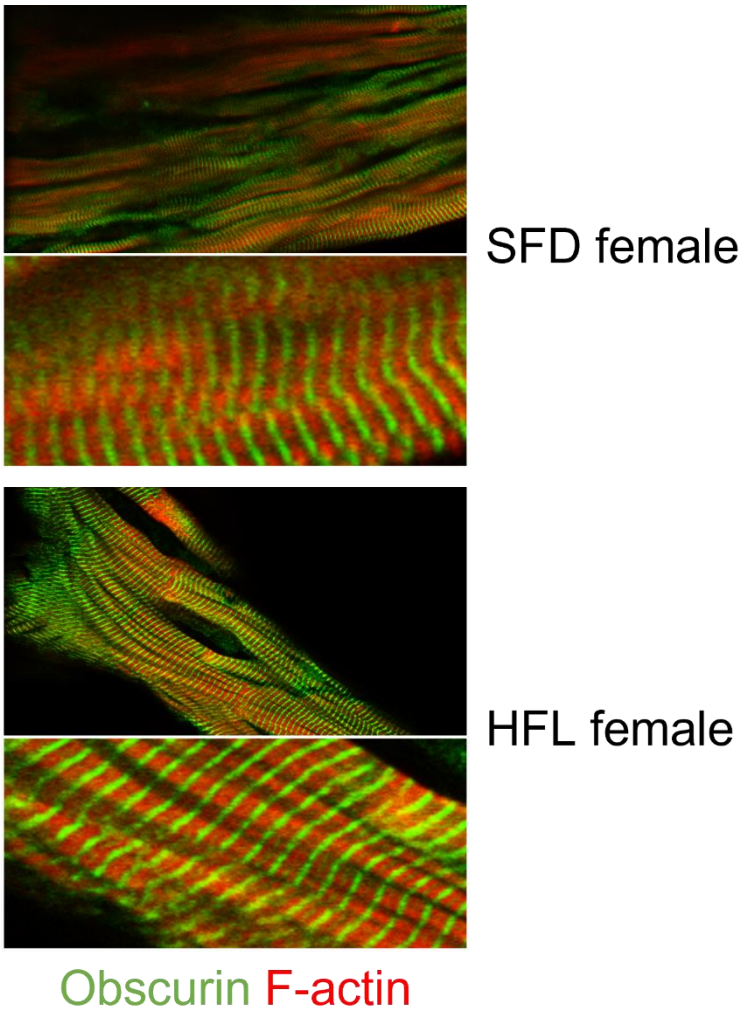

Figure 9 | 60x immunofluorescence images of obscurin. SFD – Standard fat diet mice (controls) HFL – High fat diet + L-NAME mice (test group).

Metabolic proteins

PDH was significantly ($p=0.028$) decreased (67% of female SFD) in the female HFL mice (Figure 10). Phosphorylated PDH was instead significantly ($p<0.001$ for both males and females) increased (223% for males and 206% for females) in the HFL group (Figure 10). Because of this find several additional metabolic proteins were analyzed. No changes were seen in selected glycolytic proteins (Hexokinase 1 & 2 and pyruvate kinase M 1 & 2), proteins involved in beta oxidation (Acadm and Cpt2 [Carnitine-O-palmioyltransferase 2]), ketone

metabolism (D-beta-hydroxybutyrate dehydrogenase), mitochondrial structure (sorting and assembly machinery 50 and Coiled-coil-helix-coiled-coil-helix domain containing protein 3) or in the electron transport chain (Oxaditive phosphorylation complexes 1-5 and annexin A6) (Figure 10). No significant difference in levels were found for these proteins, However, in females Pyruvate kinase M 1&2 came very close as the levels of HFL were 60% of female control levels with a p-value of 0.056 (Figure 10).

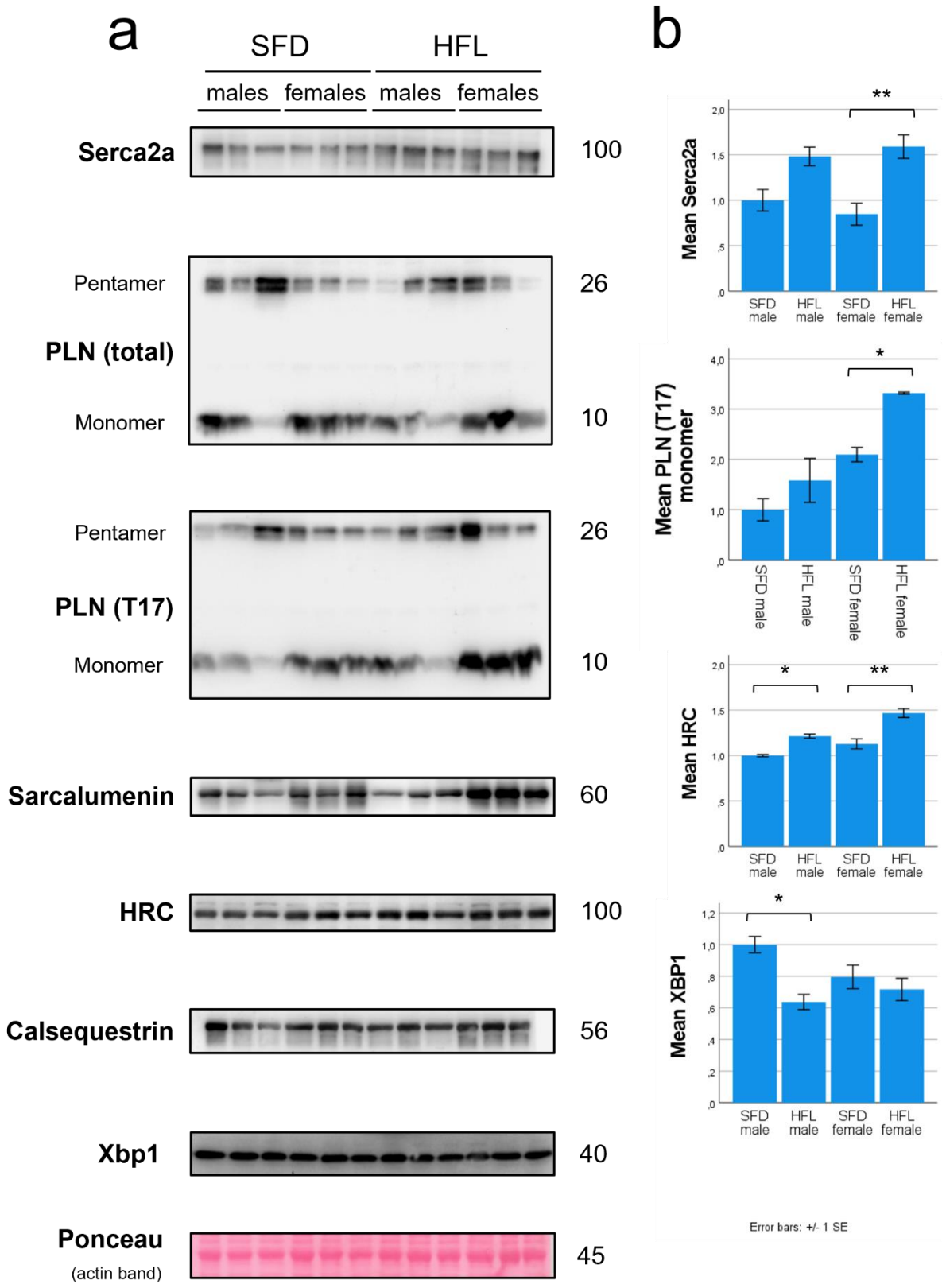

Figure 10 | **a.** Western blots of the metabolic proteins. The images have been cropped to only include the relevant bands with the molecular weight (Kilodaltons) of the protein to the right. Darker bonds correspond to a higher concentration of the protein in the sample in correlation to cardiac actin. SFD - Standard fat diet mice (control group), HFL - High fat diet + L-NAME mice (test group). The proteins analyzed are Pyruvate dehydrogenase (PDH), Phosphorylated pyruvate dehydrogenase (p-PDH), Hexokinase 1 and 2 (Hk1 & Hk2),

Pyruvate kinase M 1&2 (PKM 1/2), ? (Acadm), Carnitine O-palmitoyltransferase 2 (CPT2), D-beta-hydroxybutyrate dehydrogynase (BDH), Sorting and assembly machinery 50 (SAM50), Coiled-coil-helix-coiled-coil-helix domain containing protein 3 (CHCHD3), Oxidative phosphorylation proteins complex 1-5 (Oxphos) and Annexin A6 (Anxa6). Ponceau stained actin band is shown as loading control. **b.** Quantified values of selected western blots shown in bar graphs. *p<0.05, ***p<0.001

Proteins associated to the Sarcoplasmic Reticulum

The levels of Serca2a, a protein that transports calcium from the cytosol to the SR, were significantly (p=0.009) increased (188% of female SFD) in female HFL mice, there also was a nonsignificant (p=0.078) increase (148% of male SFD) in male HFL mice (Figure 11). No significant change of protein levels was seen in the monomeric or pentameric form of the Serca2a inhibitor Phospholamban (PLN) (Figure 11). However, a significant (p=0.038) increase (158% of SFD female) of the monomeric form of PLN-T17, the inactivated version of Phospholamban by phosphorylation at T-17, was found in female HFL mice (Figure 11). The calcium SR-storage, uptake and release associated protein HRC was significantly increased in both male (121% of male SFD, p=0.019) and female (130% of female SFD, p=0.001) mice (Figure 11). There was no significant change in protein levels of Sarcalumenin (a Serca2a modulator) and Calsequestrin (an SR calcium storage protein) between healthy and sick mice (Figure 11). Xbp1, a protein elevated by endoplasmic reticulum stress, was significantly (p=0.014) decreased (64% of SFD male) in male HFL mice. No significant change was found in the female mice (Figure 11).

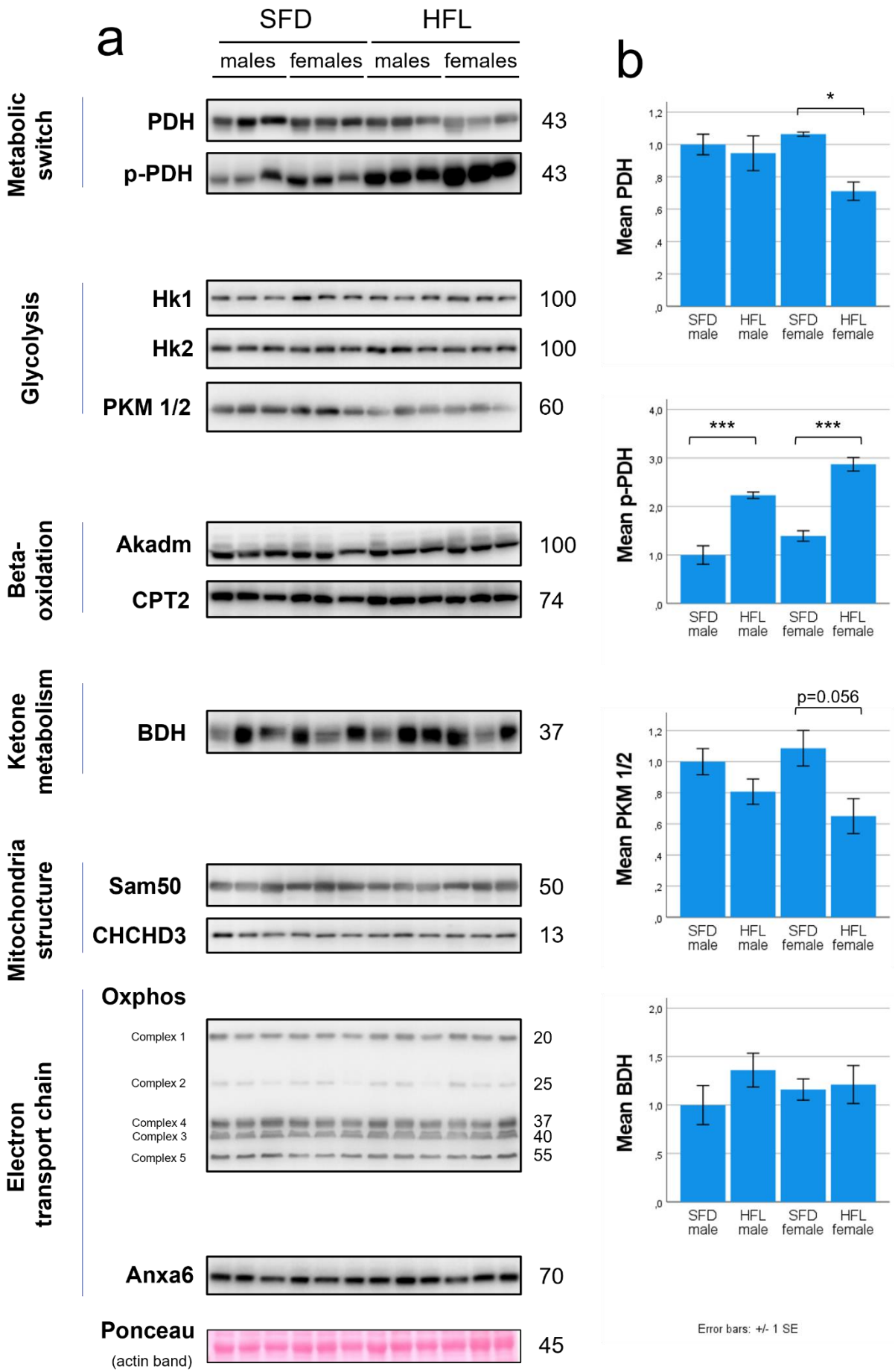
a
SFD
HFL
males
females
males
females
Metabolic switch
PDH
p-PDH
43
43
Glycolysis
Hk1
Hk2
PKM 1/2
100
100
60
Beta-oxidation
Akadm
CPT2
100
74
Ketone metabolism
BDH
37
Mitochondria structure
Sam50
CHCHD3
50
13
Electron transport chain
Oxphos
Complex 1
Complex 2
Complex 4
Complex 3
Complex 5
20
25
37
40
55
Anxa6
70
Ponceau
(actin band)
45
b
Mean PDH
*
Mean p-PDH
***
***
Mean PKM 1/2
p=0.056
Mean BDH
SFD male
HFL male
SFD female
HFL female
Error bars: +/- 1 SE

Figure 11 | **Western blots of the proteins related to the sarcoplasmic reticulum for SFD and HFL mice.** The images have been cropped to only include the relevant bands with the molecular weight (Kilodaltons) of the protein to the right. Darker bonds correspond to a higher concentration of the protein in the sample in correlation to cardiac actin. The proteins analyzed are Sarco/endoplasmic reticulum calcium (Ca2+) ATPase cardiac isoform (Serca2a), monomer and pentamer versions of Phospholamban (PLN), monomer and pentamer versions of PLN phosphorylated at Threonine-17 (PLN (T-17)), Sarcalumenin, Sarcoplasmic reticulum histidine-rich calcium-binding protein (HRC), Calsequestrin and X-box binding protein 1 (Xbp1). SFD – Standard fat diet, HFL – High fat diet + L-NAME. Ponceau stained actin band is shown as loading control. **b.** Quantified values of selected western blots shown in bar graphs. *$p<0.05$, **$p<0.01$

Discussion

Protein expression in females were more affected than in male mice.

The change in protein levels tended to be at a higher degree of significance between female SFD and HFL mice compared to between male SFD and HFL mice. Only the protein Xbp1 broke this trend by reaching significance in males but not females. This is an interesting trend considering female human patients are diagnosed with HFpEF at a larger degree than men. (3) Do female HFL mice get more affected by the treatment and is that why we see these changes in protein expression? Additional research made on the HFL model surprisingly indicate that female gender is protective for the phenotype with less lung congestion and better left ventricular function compared to male HFL mice. (14) Perhaps the changes in protein expression could be protective in general and a way for the heart to compensate the increased load of high blood pressure and obesity and not a part of the disease process.

Comparing the models

Pyruvate dehydrogenase and Pyruvate kinase as key enzyme to investigate metabolic changes

The function of pyruvate dehydrogenase is catalyzing the reaction Pyruvate → Acetyl CoA, thereby linking glycolysis to the TCA-cycle (Krebs cycle). The phosphorylation of PDH decreases the activity of the protein, allowing Acetyl-CoA generated by beta-oxidation (burning of fatty acids) to be used instead of Acetyl-CoA from the glycolysis pathway. Modulation of PDH phosphorylation is important for example during fasting. (15) Our results are therefore a sign of a decreased flow of pyruvate from the glycolytic pathway to the TCA cycle because of increased phosphorylation of PDH and, in females, also a significant decrease in overall PDH levels. This could be explained by the mice using more fat in its

metabolism, which the obese mice have plenty of. Also, HFL mice have shown to have increased glucose intolerance. (8) It is possible that the intracellular glucose levels already are elevated and the phosphorylation of PDH is a way to keep a normal metabolism. However, interestingly the opposite effect was seen in the Obscurin/Obsl1 dKO mice (Figure 2, unpublished results). The dKO mice had less phosphorylated PDH, pointing towards a metabolic switch to predominantly use glucose as its source of energy. These findings underline a main difference between the two models in their metabolic profiles.

Pyruvate kinase 1 and 2 are the enzymes of the last step of glycolysis which is also rate-limiting. While changes to PKM1/2 levels do not reach statistical significance, the level of this key glycolytic enzyme is downregulated in HFL female mice ($p=0.056$). This change indicates that not only the link of glycolysis to the Krebs cycle is inhibited, but also glycolysis itself. This two-way suppression points toward a strong suppression of glucose metabolism and fat metabolism being most prominent in the mouse model.

Ketone metabolism

We also investigated changes to ketone metabolism, as measured by BDH1 protein levels. This enzyme is important for the regulation of myocardial ketone body uptake and oxidation. BDH1 levels were found altered in the Obscurin/Obsl1 dKO mice. However, no changes to BDH1 levels were observed in HFL mice. Ketone bodies can be increasingly utilized as energy source in HF (16)

Obscurin and Obsl1

In female mice our results show that the intracellular localization of Obscurin in the sarcomere is preserved, but that the total concentration of Obscurin is reduced. The Obsl1 concentration in female mice is increased. No conclusions could be drawn from the intracellular localization of Obsl1 in high magnification (63x), as the staining was of too poor quality (data not shown). These findings combined with the fact that Obscurin/Obsl1 dKO mice develops HFpEF at least partially supports the idea that these proteins play an important role in the disease. However, it is interesting that male HFL mice only had a 20% change in expression of these proteins compared to the larger 90% increase in Obsl1 and 60% decrease in Obscurin of the female mice.

What could be causing the large change of expression in female mice? Obsl1 and Obscurin have been shown to both bind to the same binding sites in titin in the M-band protein myomesin-1. (17) Obscurin and Obsc1 has therefore been hypothesized to have redundant functions. If Obscurin is missing, Obsl1 can instead potentially bind to titin and rescue the phenotype. (11) It is possible that this is an effect seen here, whereby a decrease in one protein (Obscurin) is matched by increased expression of the other protein (Obsl1). A larger strain is placed on the heart in the disease model with increased blood pressure and fat mass, perhaps Obscurin is damaged or detached from titin because of this resulting in a decrease of concentration in the cell. Obsl1 could then compensate this loss by taking Obscurin's place in the M-band. Better quality immunofluorescent images would however be needed to show the localization of Obsl1. In addition, analysis of mRNA levels should be done to see if the change in protein level is preceded by a similar change in the levels of mRNA of both proteins.

Changes to SR and calcium cycling proteins

The results also show changes to some sarcoplasmic proteins with functions related to calcium turnover in the cardiomyocyte. Since Serca2a increased and the monomeric form of PLN-T17 decreased in females it appears that, at least in female mice, there is a change in calcium transport back into the SR. The opposite relation has been showed in failing human hearts where Serca2a has been shown to be decreased and the reuptake of calcium into the SR therefore is impaired. (18) It does not seem like this is the case in the HFL mice, but perhaps the changed Serca2a activity could be a compensatory mechanism to improve the diastolic function? There could also be other factors affecting calcium turnover that explains the Serca2a changes. We were not able to generate good quality western blots of the Ryanodine receptor responsible for the release of calcium from the SR into the cytosol which would be useful for deeper analysis of the calcium turnover in HFL cardiac cells. In addition, experiments that investigate the calcium cycling in freshly isolated cardiomyocytes using fluorescent calcium dyes (e.g. using Fluo-4 or Fura-2) would provide additional meaningful insights into changes observed in HFL mice.

Methodological considerations

The study was made on a small number of animals as there only were three mice for each group in the immunoblot experiments. This meant that it took a high magnitude change in protein expression for it to be picked up as statistically significant. Many of the proteins analyzed must be strictly regulated in the cell for its survival and might only be slightly affected in the disease model. This might especially be the case for many of the metabolic proteins analyzed as we did not see any significant change even though the diseased mice are both diabetic and obese. The same applies for the immunofluorescence analyses, as there was only one animal in each of the group studied this way.

There is a risk of confounding factors in a study like this and there is no way to be completely certain that the changes in protein levels measured are solely caused by the HFpEF disease progress. However, the mouse strain used in both the test and control group are the same (CL57BL/6) and the environmental factors is kept the same for all groups excluding the diet and hypertensive drug fed to the test group. With this approach, the possible cofounding factors should be minimal and the protein levels in each group should be normally distributed.

The analysis of the blots was made in the computer program Fiji where a densitometry graph was made from each blot. During this step the area under the curve analyzed had to be manually approximated by drawing a line at the base of the curve. During this step there could have been human error resulting in a larger or smaller area under the curve and therefore error in concentration levels of the proteins.

Additionally, some of the immunoblots were not of the best quality and will have to be repeated and confirmed to be certain that the results are correct. The reason for this were suspected to primarily be because the antibodies were of poor quality or had gone bad, and that the protein samples themselves lost a bit of quality after several freezing and defrosting cycles.

Conclusions and Implications

There were little similarities in protein expression when comparing the Obscurin/Obsl1 dKO mice to the HFL mice. HRC was lowered in the dKO model but increased in HFL, reduced phosphorylation of PLN in dKO but increased phosphorylation in HFL, Sarcalumenin was decreased in dKO while no change was seen in HFL mice and Calsequestrin was unchanged in both models. The metabolism had completely different changes with a metabolic switch towards glucose metabolism in dKO mice and an opposite switch to fat metabolism in HFL mice. Obscurin and Obsl1 showed changes only in female HFL mice, while levels of both proteins in male mice were practically unchanged. No complete loss of obscurin and/or Obsl1 (as in the dKO mice) was observed in the HFL mice. The fact that these two completely different models with different metabolic profiles and different ways of developing HFpEF also develop different changes in protein expression strongly point towards the multifactorial aspects of the disease. From what we have seen in these experiments, there is not any strong results pointing towards a common factor that connects these models and is responsible for the disease, but there are signs that Obscurin and Obsl1 is important for the pathogenesis which needs to be further studied. Also, the sarcoplasmic reticulum is affected in both models which means the calcium turnover also should be affected, perhaps in similar ways, but that remains to be experimentally verified.

Acknowledgements

Huge thanks to my supervisors Stephan Lange and Emma Börgeson for taking me on and making this project work during a global pandemic. A special thanks to Stephan for your incredible ability to explain the hard topics of our research in an easy fashion and with a passion for teaching, your patience with me in the lab and for your hard work to help me all the way from the project plan to the finalized paper.

Thanks to University of California, San Diego and the employees Mats Liu and Cindy Treich for letting me come to the university and do research in their laboratory and for helping me with the administrative work to get there.

Huge thanks to Lindhés Advokatbyrå, Sahlgrenska resestipendier and Adlerbertska stiftelser for their scholarships to make this research possible.

Thanks to Antonio Kourieh and Daniel Berhane for helping me make this project possible in the first place and making it even more enjoyable with your company.

References

1. Gangadhar TC, Von Der Lohe E, Sawada SG, Helft PR. Takotsubo cardiomyopathy in a patient with esophageal cancer: a case report. Journal of Medical Case Reports. 2008;2(1):379.
2. Virani SS, Alonso A, Aparicio HJ, Benjamin EJ, Bittencourt MS, Callaway CW, et al. Heart Disease and Stroke Statistics—2021 Update. Circulation. 2021;143(8).
3. Borlaug BA, Redfield MM. Diastolic and Systolic Heart Failure Are Distinct Phenotypes Within the Heart Failure Spectrum. Circulation. 2011;123(18):2006-14.
4. Dunlay SM, Roger VL, Redfield MM. Epidemiology of heart failure with preserved ejection fraction. Nature Reviews Cardiology. 2017;14(10):591-602.
5. McDonagh TA, Metra M, Adamo M, Gardner RS, Baumbach A, Böhm M, et al. 2021 ESC Guidelines for the diagnosis and treatment of acute and chronic heart failure. European Heart Journal. 2021;42(36):3599-726.
6. Anker SD, Butler J, Filippatos G, Ferreira JP, Bocchi E, Böhm M, et al. Empagliflozin in Heart Failure with a Preserved Ejection Fraction. New England Journal of Medicine. 2021;385(16):1451-61.
7. De Keulenaer GW, Brutsaert DL. Systolic and Diastolic Heart Failure Are Overlapping Phenotypes Within the Heart Failure Spectrum. Circulation. 2011;123(18):1996-2005.
8. Schiattarella GG, Altamirano F, Tong D, French KM, Villalobos E, Kim SY, et al. Nitrosative stress drives heart failure with preserved ejection fraction. Nature. 2019;568(7752):351-6.
9. Abou R, van der Bijl P, Bax JJ, Delgado V. Global longitudinal strain: clinical use and prognostic implications in contemporary practice. Heart. 2020;106(18):1438-44.
10. Wright N, Meyer L. Structure of giant muscle proteins. Frontiers in Physiology. 2013;4(368).
11. Lange S, Ouyang K, Meyer G, Cui L, Cheng H, Lieber RL, et al. Obscurin determines the architecture of the longitudinal sarcoplasmic reticulum. Journal of Cell Science. 2009;122(15):2640-50.
12. Blondelle J, Marrocco V, Clark M, Desmond P, Myers S, Nguyen J, et al. Murine obscurin and Obsl1 have functionally redundant roles in sarcolemmal integrity, sarcoplasmic reticulum organization, and muscle metabolism. Communications Biology. 2019;2(1).
13. Hanson D, Murray PG, Black GCM, Clayton PE. The Genetics of 3-M Syndrome: Unravelling a Potential New Regulatory Growth Pathway. Hormone Research in Paediatrics. 2011;76(6):369-78.
14. Tong D, Schiattarella GG, Jiang N, May HI, Lavandero S, Gillette TG, et al. Female Sex Is Protective in a Preclinical Model of Heart Failure With Preserved Ejection Fraction. Circulation. 2019;140(21):1769-71.
15. Gray LR, Tompkins SC, Taylor EB. Regulation of pyruvate metabolism and human disease. Cellular and Molecular Life Sciences. 2014;71(14):2577-604.
16. Rosano GM, Vitale C. Metabolic Modulation of Cardiac Metabolism in Heart Failure. Card Fail Rev. 2018;4(2):99-103.
17. Pernigo S, Fukuzawa A, Bertz M, Holt M, Rief M, Steiner RA, et al. Structural insight into M-band assembly and mechanics from the titin-obscurin-like-1 complex. Proceedings of the National Academy of Sciences. 2010;107(7):2908-13.
18. Park WJ, Oh JG. SERCA2a: a prime target for modulation of cardiac contractility during heart failure. BMB Rep. 2013;46(5):237-43.

Appendices

Recipes

15% Acrylamide gel (x1)

4.0 ml 30% Acrylamide stock
2.3 ml lower buffer
1.8 ml water
5 µl TEMED
50 µl APS

10% Acrylamide gel (x1)

2.7 ml 30% Acrylamide stock
2.3 ml lower buffer
3.0 ml water
5 µl TEMED
50 µl APS

6% Acrylamide gel (x1)

1.6 ml 30% Acrylamide stock
2.3 ml lower buffer
4.2 ml water
10 µl TEMED
100 µl APS

Stacking gel (x2)

0.6 ml acrylamide
0.9 ml upper buffer
1 ml water
30 µl Ammonium Persulfate
5 µl TEMED

TBST (1l)

9 g sodium chloride
10 ml 1M Tris HCL pH=7.4
2.5 ml 20% Tween solution
Fill with water to 1l

Blocking solution (50 ml)

10g bovine serum albumin
Fill with wash solution to 50 ml

Gold buffer
155 mM NaCl
2 mM EGTA
2 mM MgCl2
20 mM Tris-HCl
pH 7.5

Populärvetenskaplig sammanfattning

Hjärtats Proteinuttryck vid Diastolisk Hjärtsvikt i två Musmodeller

Författare:	Petter Rudbäck
Examensarbete:	30 hp
Program:	Läkarprogrammet
År:	2021
Handledare:	Stephan Lange, Emma Börgeson
Nyckelord:	HFpEF, Diastolisk hjärtsvikt, musmodell, proteinuttryck.

Diastolisk hjärtsvikt är en typ av hjärtsvikt där hjärtats pumpfunktion är bevarad men där hjärtat inte kan slappna av på ett adekvat sätt. Det är okänt vilka mekanismer som ligger bakom sjukdomen och därför har vi inte heller några bra läkemedel som kan verka mot sjukdomsprocessen och förbättra hjärtats funktion.

För att få bättre förståelse för vad som sker i sjukdomsprocessen har vi undersökt en nypublicerad musmodell av sjukdomen där möss matades med en fettrik diet och fick ett läkemedel som gav dem högt blodtryck. Vi tittade på 24 olika proteiner som är viktiga för hjärtats funktion och hur nivåerna av dessa skiljde sig från de sjuka mössen jämfört med möss som fått normal diet och var friska. Grupperna bestod av tre sjuka honmöss, tre sjuka hanmöss, tre friska honmöss och tre friska hanmöss. Det visade sig att proteinuttrycket hos de sjuka honmössen var mer påverkat än hos hanmössen, vilket tyder på att hjärtcellerna i honmössen reagerar starkare på sjukdomen. När vi jämförde de sjuka mössen mot de friska utan att ta hänsyn till kön såg vi att de sjuka mössen visade tecken på ändrad calciumomsättning i hjärtcellerna vilket är viktigt för hjärtats pump och avslappningsförmåga. Vi såg också att hjärtcellerna i mössen i större utsträckning använde fettsyror som energikälla. Slutligen så såg vi skillnader nivå av de strukturella proteinerna Obscurin och Obsl1 hos honmössen. Dessa proteiner är viktiga för att strukturerna inuti cellen ska organiseras rätt. Det

är också dessa proteiner som genom genmanipulering är borttagna i en annan musmodell av diastolisk hjärtsvikt, Obscurin/Obsl1 dubbel-knockout modellen. När vi jämförde våra resultat mot data från denna modell visade det sig att båda modellerna hade förändrad calciumomsättning i hjärtcellerna men att Obscurin/Obsl1-modellen använde mer glukos i sin energiomsättning. Detta till skillnad från modellen med fettdiet och högt blodtryck som i stället i högre utsträckning använde fett.

Sammanfattningsvis verkar det som att calciumomsättning och de strukturella proteinerna Obscurin och Obsl1 kan ha en central bakomliggande roll i diastolisk hjärtsvikt, men det behövs mer forskning för att undersöka exakt vilken roll de har i sjukdomsförloppet och för att undersöka om de kan vara bra målproteiner för nya mediciner.